

EFFECT OF POROSITY ON INTERFACIAL CONVECTIVE HEAT TRANSFER COEFFICIENT IN A PACKED BED

Marcelo B. Saito¹

Marcelo J.S. De-Lemos^{2*}

Departamento de Energia - IEME

Instituto Tecnológico de Aeronáutica - ITA

12228-900 - São José dos Campos - SP - Brasil

* Corresponding author, ¹mbsaito@mec.ita.br, ²delemos@mec.ita.br.

Abstract. Calculations utilizing the numerical solutions for the interfacial convective heat transfer coefficient with the fluid flowing through a packed bed, arbitrary bed temperature and arbitrary inlet fluid temperature have been carried out. The numerical technique employed for discretizing the governing equations is the control volume method with a boundary-fitted non-orthogonal coordinate system. The SIMPLE algorithm is used to handle the pressure-velocity coupling. The temperature distributions of the fluid and the influence of the porosity on the average heat transfer coefficient at the steady periodic state are presented.

Keywords. Porous Media, Heat Transfer Coefficient, Thermal Non-Equilibrium.

1. Introduction

The transport phenomena in porous media have been of continuing interest for last decades. This interest stems from the complicated and interesting phenomena associated with transport processes in porous media. The wide applications available have led to numerous investigations in this area. Such applications can be found in solar receiver devices, building thermal insulation, heat exchangers, energy storage units, etc. Our attention in this study focuses laminar and turbulent flow through a packed bed where represents an important configuration for efficient heat and mass transfer. A common model used for analyzing such system is the so-called "local thermal equilibrium" assumption where both solid and fluid phase temperatures are represented by a unique value. However, in many instances it is important to take into account distinct temperatures for the porous material and for the working fluid. In transient heat conduction processes, for example, the assumption of local thermal equilibrium must be discarded, according to references Kaviany (1995) and Hsu (1999). Also, when there is significant heat generation in any one of the two phases, namely solid or fluid, average temperatures are no longer identical so that the hypothesis of local thermal equilibrium must be reevaluated. This suggests the use of equations governing thermal non-equilibrium involving distinct energy balances for both the solid and fluid phases. Accordingly, the use of such two-energy equation model requires an extra parameter to be determined, namely the heat transfer coefficient between the fluid and the solid material Kuznetsov (1998).

Quintard, M., (1998) argues that assessing the validity of the assumption of local thermal equilibrium is not a simple task since the temperature difference between the two phases cannot be easily estimated. He suggests that the use of a two-energy equation model is a possible approach to solving to the problem.

Kuwahara et. al (2001) proposed a numerical procedure to determine macroscopic transport coefficients from a theoretical basis without any empiricism. They used a single unit cell and determined the interfacial heat transfer coefficient for the asymptotic case of infinite conductivity of the solid phase. Nakayama et. al (2001) extended the conduction model of Hsu (1999) for treating also convection in porous media. Having established the macroscopic energy equations for both phases, useful exact solutions were obtained for two fundamental heat transfer processes associated with porous media, namely, steady conduction in a porous slab with internal heat generation within the solid, and also, thermally developing flow through a semi-infinite porous medium.

In all of the above, only laminar flow has been considered. When treating turbulent flow in porous media, however, difficulties arise due to the fact that the flow fluctuates with time and a volumetric average is applied Gray & Lee (1977). For handling such situations, a new concept called *double decomposition* has been proposed for developing a macroscopic model for turbulent transport in porous media Pedras & de Lemos (2000) Pedras & de Lemos (2001a) Pedras & de Lemos (2001c) Pedras & de Lemos (2001b) Pedras & de Lemos (2003). This methodology has been extended to non-buoyant heat transfer Rocamora & de Lemos (2000), buoyant flows by de Lemos & Braga (2003) and mass transfer by de Lemos & Mesquita (2003). Based on this same concept, de Lemos & Rocamora (2002) have developed a macroscopic turbulent energy equation for a homogeneous, rigid and saturated porous medium, considering local thermal equilibrium between the fluid and the solid matrix. A general classification of all methodologies for treating turbulent flow and heat transfer in porous media has been recently published de Lemos & Pedras (2001).

This work proposes a macroscopic heat transfer analysis using a two-energy equation model for conduction and convection mechanisms in porous media. Saito & de Lemos (2004) proposed an extension of the transport model of de

Lemos & Rocamora (2002) considers local thermal non-equilibrium. The contribution herein consists in documenting and testing a detailed numerical model for obtaining the interfacial heat transfer coefficient for variable porosity.

2. Microscopic Transport Equations

Microscopic transport equations for incompressible fluid flow in a rigid homogeneous porous medium have been already presented in the literature and for that they are here just presented (e.g. reference de Lemos & Rocamora (2002)). They read,

$$\text{Continuity: } \nabla \cdot \mathbf{u} = 0. \quad (1)$$

$$\text{Momentum: } \mathbf{r} \left[\frac{\partial \mathbf{u}}{\partial t} + \nabla \cdot (\mathbf{u}\mathbf{u}) \right] = -\nabla p + \mathbf{m} \nabla^2 \mathbf{u}. \quad (2)$$

$$\text{Energy - Fluid Phase: } (\mathbf{r} c_p)_f \left\{ \frac{\partial T_f}{\partial t} + \nabla \cdot (\mathbf{u} T_f) \right\} = \nabla \cdot (k_f \nabla T_f) + S_f. \quad (3)$$

$$\text{Energy - Solid Phase (Porous Matrix): } (\mathbf{r} c_p)_s \frac{\partial T_s}{\partial t} = \nabla \cdot (k_s \nabla T_s) + S_s. \quad (4)$$

where the subscripts f and s refer to fluid and solid phases, respectively. Here, \mathbf{r} is the fluid density, \mathbf{u} is the fluid instantaneous velocity, p is the pressure, \mathbf{m} represents the fluid viscosity, T is the temperature k_f is the fluid thermal conductivity, k_s is the solid thermal conductivity, c_p is the specific heat and S is the heat generation term. If there is no heat generation either in the solid or in the fluid, one has further $S_f = S_s = 0$.

3. Decomposition of Flow Variables in Space and Time

Macroscopic transport equations for turbulent flow in a porous medium are obtained through the simultaneous application of time and volume average operators over a generic fluid property \mathbf{j} Gray & Lee (1977). Such concepts are mathematically defined as,

$$\bar{\mathbf{j}} = \frac{1}{\Delta t} \int_t^{t+\Delta t} \mathbf{j} dt, \text{ with } \mathbf{j} = \bar{\mathbf{j}} + \mathbf{j}' \quad (5)$$

$$\langle \mathbf{j} \rangle^i = \frac{1}{\Delta V_f} \int_{\Delta V_f} \mathbf{j} dV; \langle \mathbf{j} \rangle^v = \mathbf{f} \langle \mathbf{j} \rangle^i; \mathbf{f} = \frac{\Delta V_f}{\Delta V}, \text{ with } \mathbf{j} = \langle \mathbf{j} \rangle^i + {}^i \mathbf{j} \quad (6)$$

where ΔV_f is the volume of the fluid contained in a Representative Elementary Volume (REV) ΔV .

The *double decomposition* idea introduced and fully described in Pedras & de Lemos (2000) Pedras & de Lemos (2001a) Pedras & de Lemos (2001c) Pedras & de Lemos (2001b) Pedras & de Lemos (2003), combines Eqs. (5)-(6) and can be summarized as:

$$\overline{\langle \mathbf{j} \rangle^i} = \langle \bar{\mathbf{j}} \rangle^i; {}^i \bar{\mathbf{j}} = \overline{{}^i \mathbf{j}}; \langle \mathbf{j} \rangle^i = \langle \mathbf{j} \rangle^i \quad (7)$$

and,

$$\left. \begin{array}{l} \mathbf{j}' = \langle \mathbf{j} \rangle^i + {}^i \mathbf{j}' \\ {}^i \mathbf{j} = \overline{{}^i \mathbf{j}} + {}^i \mathbf{j}' \end{array} \right\} \text{ where } {}^i \mathbf{j}' = \mathbf{j}' - \langle \mathbf{j} \rangle^i = {}^i \mathbf{j} - \overline{{}^i \mathbf{j}}. \quad (8)$$

Therefore, the quantity \mathbf{j} can be expressed by either,

$$\mathbf{j} = \overline{\langle \mathbf{j} \rangle^i} + \langle \mathbf{j} \rangle^i + \overline{{}^i \mathbf{j}} + {}^i \mathbf{j}', \quad (9)$$

or

$$\mathbf{j} = \langle \bar{\mathbf{j}} \rangle^i + {}^i \bar{\mathbf{j}} + \langle \mathbf{j} \rangle^i + {}^i \mathbf{j}'. \quad (10)$$

The term ${}^i \mathbf{j}'$ can be viewed as either the temporal fluctuation of the spatial deviation or the spatial deviation of the temporal fluctuation of the quantity \mathbf{j} .

4. Macroscopic Flow and Energy Equations

When the average operators (5)-(6) are applied over Eqs. (1)-(2), macroscopic equations for turbulent flow are obtained. Volume integration is performed over a Representative Elementary Volume (REV), Gray & Lee (1977) and Slattery (1967) resulting in,

$$\text{Continuity: } \nabla \cdot \bar{\mathbf{u}}_D = 0. \quad (11)$$

where, $\bar{\mathbf{u}}_D = \mathbf{f}\langle\bar{\mathbf{u}}\rangle^i$ and $\langle\bar{\mathbf{u}}\rangle^i$ identifies the intrinsic (liquid) average of the time-averaged velocity vector $\bar{\mathbf{u}}$.

Momentum:

$$\mathbf{r} \left[\frac{\partial \bar{\mathbf{u}}_D}{\partial t} + \nabla \cdot \left(\frac{\bar{\mathbf{u}}_D \bar{\mathbf{u}}_D}{\mathbf{f}} \right) \right] = -\nabla(\mathbf{f}\langle\bar{p}\rangle^i) + \mathbf{m} \nabla^2 \bar{\mathbf{u}}_D - \nabla \cdot (\mathbf{r} \mathbf{f} \langle \overline{\mathbf{u}'\mathbf{u}'} \rangle^i) - \left[\frac{\mathbf{m}\mathbf{f}}{K} \bar{\mathbf{u}}_D + \frac{c_F \mathbf{f} \mathbf{r} \bar{\mathbf{u}}_D / \bar{\mathbf{u}}_D}{\sqrt{K}} \right], \quad (12)$$

where the last two terms in Eq. (12), represent the Darcy and Forchheimer contributions by Forchheimer (1901). The symbol K is the porous medium permeability, c_F is the form drag or Forchheimer coefficient, $\langle\bar{p}\rangle^i$ is the intrinsic average pressure of the fluid, and \mathbf{f} is the porosity of the porous medium.

The macroscopic Reynolds stress $-\mathbf{r} \mathbf{f} \langle \overline{\mathbf{u}'\mathbf{u}'} \rangle^i$ appearing in Eq. (12) is given as,

$$-\mathbf{r} \mathbf{f} \langle \overline{\mathbf{u}'\mathbf{u}'} \rangle^i = \mathbf{m}_f 2 \langle \bar{\mathbf{D}} \rangle^v - \frac{2}{3} \mathbf{f} \mathbf{r} \langle k \rangle^i \mathbf{I}, \quad (13)$$

where,

$$\langle \bar{\mathbf{D}} \rangle^v = \frac{1}{2} \left[\nabla(\mathbf{f}\langle\bar{\mathbf{u}}\rangle^i) + [\nabla(\mathbf{f}\langle\bar{\mathbf{u}}\rangle^i)]^T \right], \quad (14)$$

is the macroscopic deformation tensor, $\langle k \rangle^i = \langle \overline{\mathbf{u}'\mathbf{u}'} \rangle^i / 2$ is the intrinsic turbulent kinetic energy, and \mathbf{m}_f , is the turbulent viscosity, which is modeled in de Lemos & Pedras (2001) similarly to the case of clear flow, in the form,

$$\mathbf{m}_f = \mathbf{r} c_m \frac{\langle k \rangle^i}{\langle \mathbf{e} \rangle^i}, \quad (15)$$

The intrinsic turbulent kinetic energy per unit mass and its dissipation rate are governed by the following equations,

$$\mathbf{r} \left[\frac{\partial}{\partial t} (\mathbf{f}\langle k \rangle^i) + \nabla \cdot (\bar{\mathbf{u}}_D \langle k \rangle^i) \right] = \nabla \cdot \left[\left(\mathbf{m} + \frac{\mathbf{m}_f}{\mathbf{s}_k} \right) \nabla (\mathbf{f}\langle k \rangle^i) \right] - \mathbf{r} \langle \overline{\mathbf{u}'\mathbf{u}'} \rangle^i : \nabla \bar{\mathbf{u}}_D + c_k \mathbf{r} \frac{\mathbf{f}\langle k \rangle^i \bar{\mathbf{u}}_D}{\sqrt{K}} - \mathbf{r} \mathbf{f} \langle \mathbf{e} \rangle^i. \quad (16)$$

$$\begin{aligned} \mathbf{r} \left[\frac{\partial}{\partial t} (\mathbf{f}\langle \mathbf{e} \rangle^i) + \nabla \cdot (\bar{\mathbf{u}}_D \langle \mathbf{e} \rangle^i) \right] = \\ \nabla \cdot \left[\left(\mathbf{m} + \frac{\mathbf{m}_f}{\mathbf{s}_e} \right) \nabla (\mathbf{f}\langle \mathbf{e} \rangle^i) \right] + c_1 (-\mathbf{r} \langle \overline{\mathbf{u}'\mathbf{u}'} \rangle^i : \nabla \bar{\mathbf{u}}_D) \frac{\langle \mathbf{e} \rangle^i}{\langle k \rangle^i} + c_2 c_k \mathbf{r} \frac{\mathbf{f}\langle \mathbf{e} \rangle^i \bar{\mathbf{u}}_D}{\sqrt{K}} - c_2 \mathbf{r} \mathbf{f} \frac{\langle \mathbf{e} \rangle^i}{\langle k \rangle^i}. \end{aligned} \quad (17)$$

where, c_k , c_1 , c_2 and c_m are nondimensional constants.

Similarly, macroscopic energy equations are obtained for both fluid and solid phases by applying time and volume average operators to Eqs. (3)- (4). As in the flow case, volume integration is performed over a Representative Elementary Volume (REV) resulting in,

$$\begin{aligned} (\mathbf{r} c_p)_f \left[\frac{\partial \mathbf{f}\langle \overline{T}_f \rangle^i}{\partial t} + \nabla \cdot \left\{ \mathbf{f} \left(\langle \bar{\mathbf{u}} \rangle^i \langle \overline{T}_f \rangle^i + \langle \bar{\mathbf{u}} \rangle^i \overline{T}_f' + \langle \bar{\mathbf{u}}' \rangle^i \overline{T}_f \right) \right\} \right] = \nabla \cdot \left[k_f \nabla (\mathbf{f}\langle \overline{T}_f \rangle^i) \right] + \\ \nabla \cdot \left[\frac{1}{\Delta V} \int_{A_i} \mathbf{n}_i k_f \overline{T}_f dA \right] + \frac{1}{\Delta V} \int_{A_i} \mathbf{n}_i \cdot k_f \nabla \overline{T}_f dA \end{aligned} \quad (18)$$

$$(\mathbf{r} c_p)_s \left[\frac{\partial (1-\mathbf{f})\langle \overline{T}_s \rangle^i}{\partial t} \right] = \nabla \cdot \left\{ k_s \nabla [(1-\mathbf{f})\langle \overline{T}_s \rangle^i] \right\} - \nabla \cdot \left[\frac{1}{\Delta V} \int_{A_i} \mathbf{n}_i k_s \overline{T}_s dA \right] - \frac{1}{\Delta V} \int_{A_i} \mathbf{n}_i \cdot k_s \nabla \overline{T}_s dA, \quad (19)$$

where $\langle \overline{T}_s \rangle^i$ and $\langle \overline{T}_f \rangle^i$ denote the intrinsically averaged temperature of solid and fluid phases, respectively, A_i is the interfacial area within the REV and \mathbf{n}_i is the unit vector normal to the fluid-solid interface, pointing from the fluid towards the solid phase. Eqs. (18) and (19) are the macroscopic energy equations for the fluid and the porous matrix (solid), respectively.

Further, using the *double decomposition* concept, Rocamora & de Lemos (2000) have shown that the fourth term on the left hand side of Eq. (18) can be expressed as:

$$\langle \overline{\mathbf{u}'\mathbf{u}'} \rangle^i = \langle (\langle \bar{\mathbf{u}} \rangle^i + \langle \bar{\mathbf{u}}' \rangle^i) (\langle \overline{T}_f' \rangle^i + \langle \overline{T}_f \rangle^i) \rangle^i = \langle \bar{\mathbf{u}} \rangle^i \langle \overline{T}_f' \rangle^i + \langle \bar{\mathbf{u}}' \rangle^i \langle \overline{T}_f \rangle^i. \quad (20)$$

Therefore, in view of Eq. (20), Eq. (18) can be rewritten as:

$$\begin{aligned}
 (\mathbf{r} c_p)_f \left[\frac{\partial \mathbf{f} \langle \overline{T_f} \rangle^i}{\partial t} + \nabla \cdot \left\{ \mathbf{f} \left(\langle \overline{\mathbf{u}} \rangle^i \langle \overline{T_f} \rangle^i + \langle \overline{\mathbf{u}}^i \overline{T_f} \rangle^i + \langle \overline{\mathbf{u}} \rangle^i \langle \overline{T_f'} \rangle^i + \langle \overline{\mathbf{u}}^i \overline{T_f'} \rangle^i \right) \right\} \right] = \\
 \nabla \cdot \left[k_f \nabla (\mathbf{f} \langle \overline{T_f} \rangle^i) \right] + \nabla \cdot \left[\frac{1}{\Delta V} \int_{A_i} \mathbf{n}_i k_f \overline{T_f} dA \right] + \frac{1}{\Delta V} \int_{A_i} \mathbf{n}_i \cdot k_f \nabla \overline{T_f} dA
 \end{aligned} \tag{21}$$

5. Interfacial Heat Transfer Coefficient

In Eqs. (19) and (21) the heat transferred between the two phases can be modeled by means of a film coefficient h_i such that,

$$h_i a_i (\langle \overline{T_s} \rangle^i - \langle \overline{T_f} \rangle^i) = \frac{1}{\Delta V} \int_{A_i} \mathbf{n}_i \cdot k_f \nabla \overline{T_f} dA = \frac{1}{\Delta V} \int_{A_i} \mathbf{n}_i \cdot k_s \nabla \overline{T_s} dA. \tag{22}$$

where, h_i is known as the interfacial convective heat transfer coefficient and $a_i = A_i/\Delta V$ is the surface area per unit volume and A_i is the interfacial heat transfer area.

For determining h_i , Kuwahara et. al (2001) modeled a porous medium by considering an infinite number of solid square rods of size D , arranged in a regular triangular pattern (see Fig. (1)). They numerically solved the governing equations in the void region, exploiting to advantage the fact that for an infinite and geometrically ordered medium a repetitive cell can be identified. Periodic boundary conditions were then applied for obtaining the temperature distribution under fully developed flow conditions. A numerical correlation for the interfacial convective heat transfer coefficient was proposed by Kuwahara et. al (2001) as,

$$\frac{h_i D}{k_f} = \left(1 + \frac{4(1-f)}{f} \right) + \frac{1}{2} (1-f)^{1/2} Re_D Pr^{1/3}, \text{ valid for } 0.2 < f < 0.9, \tag{23}$$

Eq. (23) is based on porosity dependency and is valid for packed beds of particle diameter D .

This same physical model will be used here for obtaining the interfacial heat transfer coefficient h_i for macroscopic flows.

6. Periodic Cell and Boundary Conditions

In order to evaluate the numerical tool to be used in the determination of the film coefficient given by Eq. (22), a test case was run for obtaining the flow field in a periodic cell, which is here assumed to represent the porous medium. Consider a macroscopically uniform flow through an infinite number of square rods of lateral size D , placed in a staggered fashion and maintained at constant temperature T_w . The periodic cell or representative elementary volume, ΔV , is schematically showed in Fig. (1) and has dimensions $2H \times H$. Computations within this cell were carried out using a non-uniform grid of size 90×70 nodes, as shown in Fig. (2), to ensure that the results were grid independent. The Reynolds number $Re_D = \mathbf{r} \mathbf{u}_D D / \mathbf{m}$ was varied from 4 to 400 and the porosity, $f = 1 - (D/H)^2$.

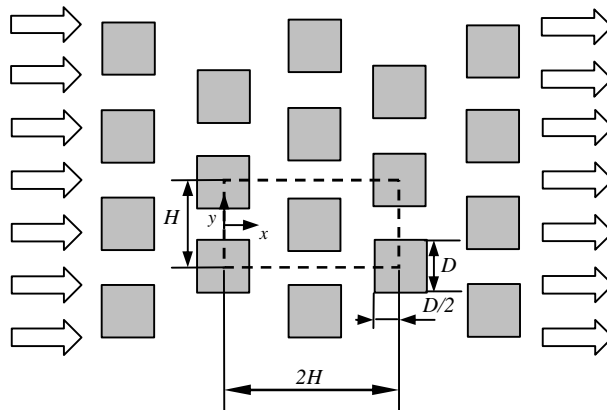


Figure 1. Physical model and coordinate system.

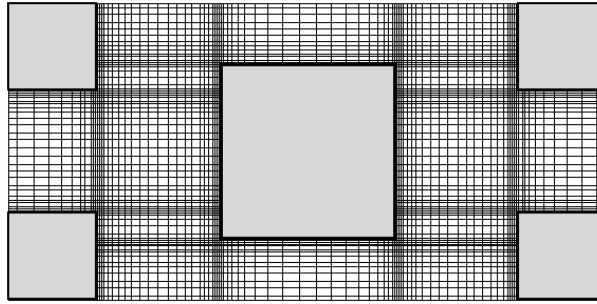


Figure 2. Non uniform computational grid.

The numerical method utilized to discretize the microscopic flow and energy equations in the unit cell is the Control Volume. The SIMPLE method of Patankar (1980) was used for the velocity-pressure coupling. Convergence was monitored in terms of the normalized residue for each variable. The maximum residue allowed for convergence check was set to 10^{-9} , being the variables normalized by appropriate reference values.

For fully developed flow in the cell of Fig. (1), the velocity at exit ($x/H = 2$) must be identical to that at the inlet ($x/H = 0$). Temperature profiles, however, are only identical at both cell exit and inlet if presented in terms of an appropriate non-dimensional variable. The situation is analogous to the case of forced convection in a channel with isothermal walls. Thus, boundary conditions and periodic constraints are given by:

On the solid walls:

$$\mathbf{u} = 0, \quad T = T_w. \quad (24)$$

On the periodic boundaries:

$$\mathbf{u}|_{inlet} = \mathbf{u}|_{outlet}, \quad (25)$$

$$\int_0^H u \, dy \Big|_{inlet} = \int_0^H u \, dy \Big|_{outlet} = H|\mathbf{u}_D|, \quad (26)$$

$$\mathbf{q}|_{inlet} = \mathbf{q}|_{outlet} \Leftrightarrow \frac{T - T_w}{T_B(x) - T_w} \Big|_{inlet} = \frac{T - T_w}{T_B(x) - T_w} \Big|_{outlet}, \quad (27)$$

The bulk mean temperature of the fluid is given by:

$$T_B(x) = \frac{\int u T \, dy}{\int u \, dy} \quad (28)$$

Computations are based on the Darcy velocity, the length of structural unit H and the temperature difference ($T_B(x) - T_w$), as references scales.

7. Preliminary Laminar Results and Discussion

7.1 Periodic Flow

Preliminary results for velocity and temperature fields were obtained for different Reynolds numbers. In order to assure that the flow is hydrodynamically and thermally developed in the periodic cell of Fig. (1), the governing equations were solved repetitively in the cell, taking the outlet profiles for \mathbf{u} and \mathbf{q} at exit and plugging them back at inlet. In the first run, uniform velocity and temperature profiles were set at the cell entrance for $Pr = 1$ and $Re_D = 100$, giving $\mathbf{q} = 1$ at $x/H = 0$. Then, after convergence of the flow and temperature fields, \mathbf{u} and \mathbf{q} at $x/H = 2$ were used as inlet profiles for a second run, corresponding to solving again the flow for a similar cell beginning in $x/H = 2$. Similarly, a third run was carried out and again outlet results, this time corresponding to an axial position $x/H = 4$, were recorded. This procedure was repeated several times until \mathbf{u} and \mathbf{q} did not differ substantially at both inlet and outlet positions. Resulting non-dimensional temperature profiles are shown in Fig. (3) showing that the periodicity constraints imposed by Eqs. (25)-(27) was satisfied for $x/H > 4$. For the entrance region ($0 < x/H < 4$), \mathbf{q} profiles change with length x/H being essentially invariable after this distance. Under this condition of constant \mathbf{q} profile, the flow was considered to be macroscopically developed for Re_D up to 400.

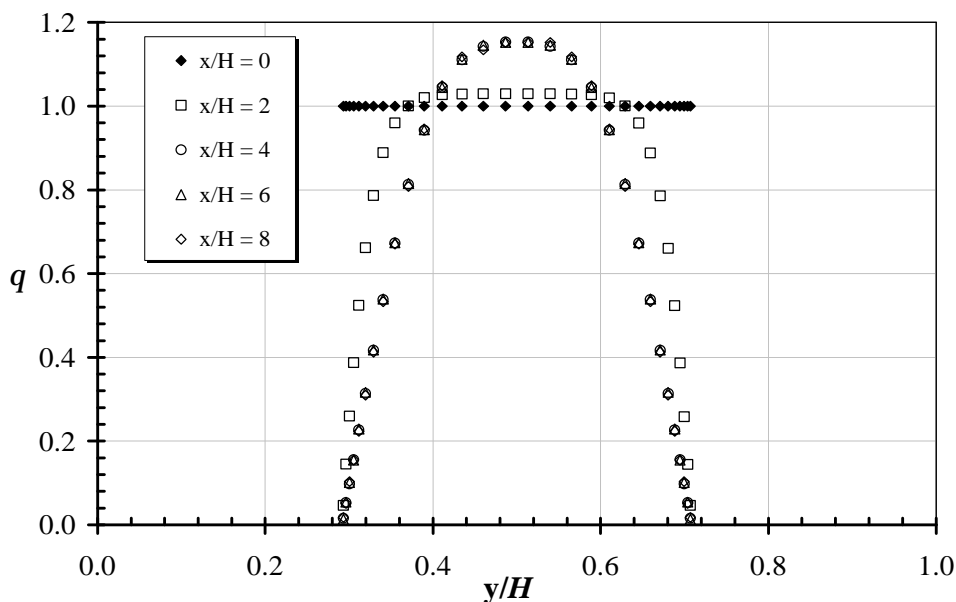


Figure 3. Dimensionless temperature profile for $Pr = 1$ and $Re_D = 100$.

7.2 Developed Flow and Temperature Fields

Macroscopically developed flow field for $Pr = 1$ and $Re_D = 100$ is presented in Fig. (4), corresponding to $x/D=6$ at the cell inlet (see Fig. (3)). The expression “macroscopically developed” is used herein to account for the fact that periodic flow has been achieved at that axial position. Figure (4) indicates that the flow impinges on the left face of the obstacles, surrounds the rod faces and forms a weak recirculation bubble past the rod. When the Reynolds number is low (not shown here), the horizontal velocity field in between two rods appears to be very similar to what we observe in a channel, namely the parabolic profile, particularly at inlet and outlet of unit cell. As Re_D increases, stronger recirculation bubbles appear further behind the rods. Temperature distribution pattern is shown in Fig. (5) and Fig. (6), also for $Re_D = 100$. Colder fluid impinges on the left surface yielding strong temperature gradients on that face. Downstream the obstacle, fluid recirculation smoothes temperature gradients and deforms isotherms within the mixing region. When the Reynolds number is sufficiently high (not shown here), the thermal boundary layers covering the rod surfaces indicate that convective heat transfer overwhelms thermal diffusion.

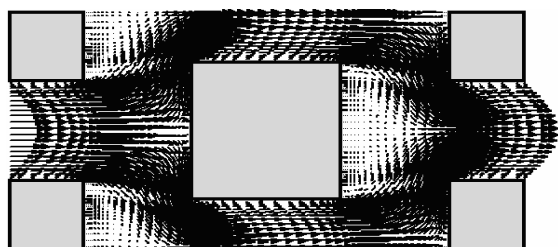


Figure 4. Velocity field for $Pr = 1$ and $Re_D = 100$.

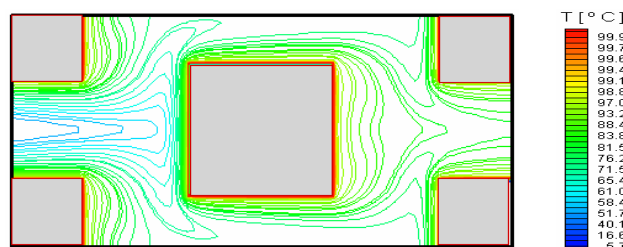


Figure 5. Isotherms for $Pr = 1$, $Re_D = 100$ and $f = 0.65$

Figure (6) shows the periodic cells used to calculate the interfacial convective heat transfer coefficient h_i . The porosity is described for each periodic cell. Therefore, $f = 0.65$ is represented in Fig. (5); $f = 0.44$; $f = 0.55$; $f = 0.75$ and $f = 0.90$ are represented in Fig. (6a); (6b); (6c) and (6d) respectively.

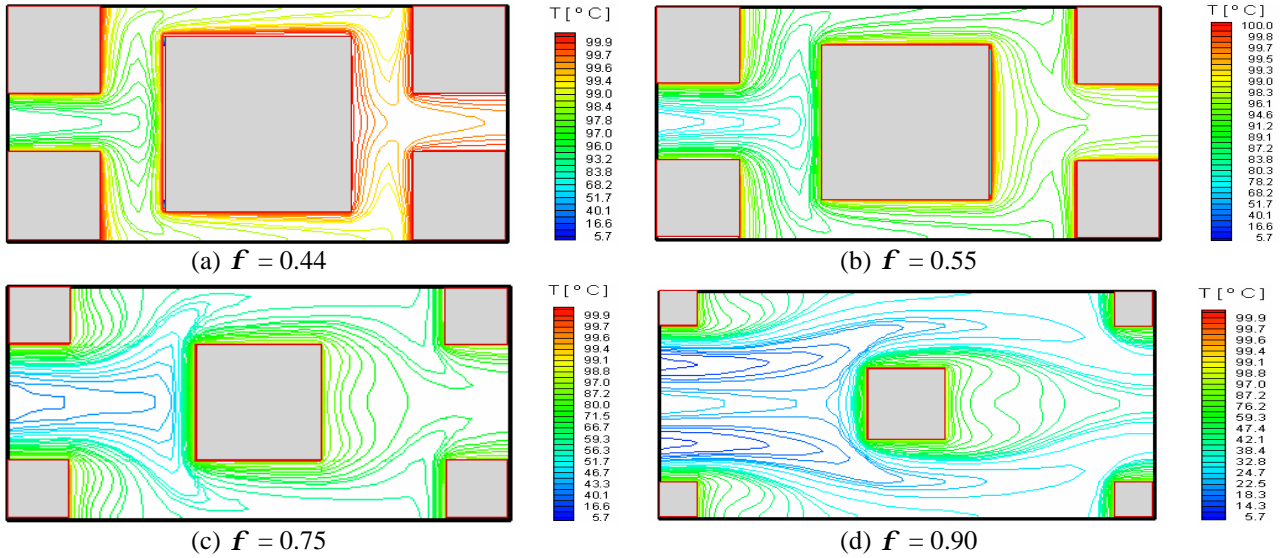


Figure 6. Isotherms for $Pr=1$ and $Re_D = 100$.

7.3 Film Coefficient h_i

Determination of h_i is here obtained by calculating, for the unit cell of Fig. (1), an expression given as,

$$h_i = \frac{Q_{total}}{A_i \Delta T_{ml}} \tag{29}$$

where $A_i = 8D \times 1$. The overall heat transferred in the cell, Q_{total} , is giving by,

$$Q_{total} = (H - D) \mathbf{r} \mathbf{u}_B c_p (T_B|_{outlet} - T_B|_{inlet}), \tag{30}$$

where \mathbf{u}_B is the bulk mean velocity of the fluid and the logarithm mean temperature difference, ΔT_{ml} is,

$$\Delta T_{ml} = \frac{(T_w - T_B|_{outlet}) - (T_w - T_B|_{inlet})}{\ln\left[\frac{(T_w - T_B|_{outlet})}{(T_w - T_B|_{inlet})}\right]} \tag{31}$$

Eq. (29) represents an overall heat balance on the entire cell and associates the heat transferred to the fluid to a suitable temperature difference ΔT_{ml} . As mentioned earlier, Eqs. (1)-(4) were numerically solved in the unit cell until conditions Eqs. (25)-(27) were satisfied.

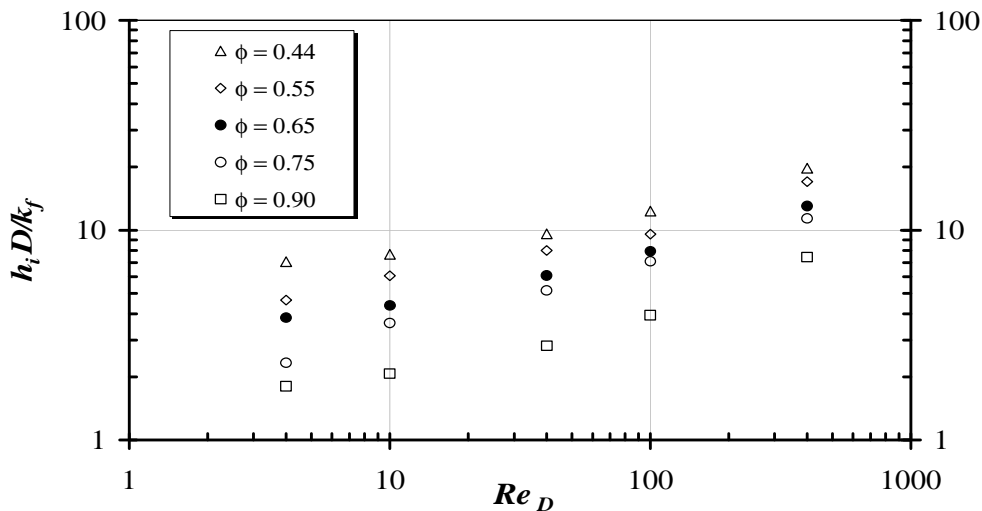


Figure 7. Effect of Re_D on h_i for $Pr=1$.

Once fully developed flow and temperature are fields are achieved, for the fully developed condition ($x > 6H$), bulk temperatures were calculated according to Eq. (28), at both inlet and outlet positions. They were then used to calculate h_i using Eqs. (29)-(31). Results for h_i are plotted in Fig. (7) and Fig. (8) for Re_D up to 400. Also plotted in

this figure are results computed with correlation (23) using $f = 0.65$. The figure seems to indicate that both computations show a reasonable agreement.

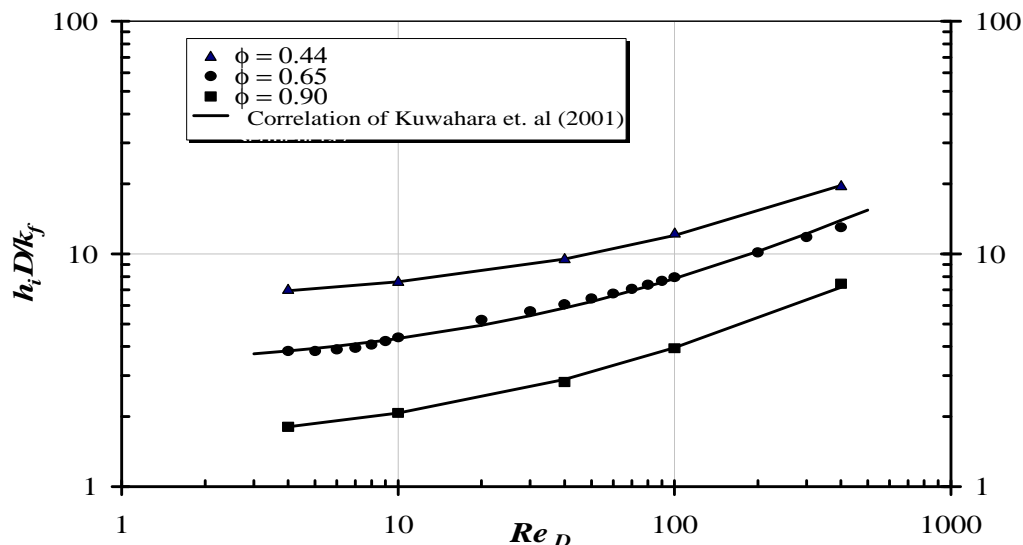


Figure 8. Effect of Re_D on h_i for $Pr = 1$ with correlation of Kuwahara *et. al* (2001) and variable porosity.

8. Concluding remarks

For a porous medium, a computational procedure for determining the convective coefficient of heat exchange between the porous substrate and the working fluid was detailed. As a preliminary result, a macroscopically uniform laminar flow through a periodic model of isothermal square rods was computed, considering periodic velocity and temperature fields. Quantitative agreement was obtained when comparing the preliminary results herein with simulations by Kuwahara *et. al* (2001)]. Further work will be carried out in order to simulate fully turbulent flow and heat transfer in porous media by means of the proposed two-energy equation. Ultimately, it is expected that a correlation for the heat transfer coefficient be obtained so that the exchange energy between the solid and the fluid can be accounted for.

9. Acknowledgements

The authors are thankful to FAPESP and CNPq Brazil, for their financial support during the course of this research.

10. References

- de Lemos, M.J.S., Pedras, M.H.J., "Recent mathematical models for turbulent flow in saturated rigid porous media", *Journal of Fluids Engineering*, 2001, 123 (4), 935 – 940.
- de Lemos, M.J.S., Braga, E.J., "Modeling of turbulent natural convection in porous media", *International Communications in Heat and Mass Transfer*, 2003, 30 (5), 615 – 624.
- de Lemos, M.J.S., Mesquita, M.S., "Turbulent mass transport in saturated rigid porous media", *International Communications in Heat and Mass Transfer*, 2003, 30 (1), 105 – 115.
- de Lemos, M.J.S., Rocamora Jr, F.D., "Turbulent Transport Modeling for Heated Flow in Rigid Porous Media", *Proc. of IHTC12 - 12th International Heat Transfer Conference, Grenoble, França, 18-23 August 2002*.
- Forchheimer, P., 1901, "Wasserbewegung durch Boden", *Z. Ver. Deutsch. Ing.*, vol. 45, pp. 1782-1788.
- Gray, W. G. & Lee, P. C. Y., "On the theorems for local volume averaging of multiphase system", *Int. J. Multiphase Flow*, vol. 3, pp. 333-340, 1977.
- Hsu, C.T., 1999, "A Closure Model for Transient Heat Conduction in Porous Media", *J. Heat Transfer* 121. pp. 733-739.
- Kaviany, M., 1995, "Principles of Heat Transfer in Porous Media", 2nd ed., Springer, New York, pp. 391-424.
- Kuznetsov, A.V., 1998, "Thermal Nonequilibrium Forced Convection in Porous Media", in D. B. Ingham and I. Pop (eds.), *Transport Phenomena in Porous Media*, Elsevier Sc., Oxford., pp. 103-129.
- Kuwahara, F., Shirota, M., Nakayama, A., 2001, "A Numerical Study of Interfacial Convective Heat Transfer Coefficient in Two-Energy Equation Model for Convection in Porous Media", *Int. J. Heat Mass Transfer* 44. pp. 1153-1159.

- Nakayama, A., Kuwahara, F., Sugiyama, M., Xu, G., 2001, "A Two-Energy Equation Model for Conduction and Convection in Porous Media", *Int. J. Heat Mass Transfer* 44. pp. 4375-4379.
- Patankar, S.V., 1980, "Numerical Heat Transfer and Fluid Flow", Mc-Graw Hill.
- Pedras, M.H.J., de Lemos, M.J.S., "On the definition of turbulent kinetic energy for flow in porous media", *International Communications in Heat and Mass Transfer*, 2000, 27 (2), 211 – 220.
- Pedras, M.H.J., de Lemos, M.J.S., "Macroscopic turbulence modeling for incompressible flow through undeformable porous media", *International Journal of Heat and Mass Transfer*, 2001a, 44 (6), 1081 – 1093.
- Pedras, M.H.J., de Lemos, M.J.S., "Simulation of turbulent flow in porous media using a spatially periodic array and a low Reynolds two-equation closure", *Numerical Heat Transfer Part A – Applications*, 2001b, 39 (1).
- Pedras, M.H.J., de Lemos, M.J.S., "On the mathematical description and simulation of turbulent flow in a porous medium formed by an array of elliptic rods", *Journal of Fluids Engineering*, 2001c, 123 (4), 941 – 947.
- Pedras, M.H.J., de Lemos, M.J.S., "Computation of turbulent flow in porous media using a Low Reynolds $k - \epsilon$ model and an infinite array of transversally-displaced elliptic rods", *Numerical Heat Transfer Part A – Applications*, 2003, 43 (6), 585 – 602.
- Quintard, M., 1998, "Modelling Local Non-Equilibrium Heat Transfer in Porous Media", in, *Proceedings of the Eleventh International Heat Transfer Conference*, Kyongju, Korea, vol. 1, pp. 279-285.
- Rocamora Jr, F.D., de Lemos, M.J.S., "Analysis of convective heat transfer for turbulent flow in saturated porous media", *International Communications in Heat and Mass Transfer*, 2000, 27 (6), 825-834.
- Saito, M.B., de Lemos, M.J.S., "Interfacial Heat Transfer Coefficient for Non-Equilibrium Convective Transport In Porous Media", *International Communications in Heat and Mass Transfer*, 2004 (submitted).
- Slattery, J. C., "Flow of viscoelastic fluids through porous media", *A.I.Ch.E. J.*, vol. 13, pp. 1066-1071, 1967.